# DETC2019-97761

## OPTIMIZATION OF EDGE GEOMETRY OF CYLINDRICAL MILLING TOOLS TO ENHANCE DYNAMIC STABILITY

**Zoltan Dombovari**\*
Department of Applied Mechanics
Budapest University of Technology and Economics
Budapest, H-1521
Hungary
Email: dombovari@mm.bme.hu

**Daniel Bachrathy, Gabor Stepan**
Department of Applied Mechanics
Budapest University of Technology and Economics
Budapest, H-1521
Hungary
Email: stepan@mm.bme.hu

## ABSTRACT

Tool geometry directly influences the dynamic performance of milling operations. Both surface properties and stability behavior are significantly influenced by the regeneration effect. The regeneration phenomenon is modelled by delay differential equations with delays originated from the time passed between consecutive flute passes. This work presents the implementation study of a constrained general optimization scheme for cutting edges of cylindrical milling cutters based on functional minimization principle. Mathematically, this leads to the determination of the corresponding weight function of a distributed delay differential equation. The presented semi-analytical methodology is based on the general milling model implemented in the semidiscretization framework.

## INTRODUCTION

This work establishes the main mathematical framework for custom tool optimization against chatter vibration. The resulted performance are expected to go further as the one for variable pitch [1], variable helix [2] or serrated cylindrical tools [3]. This broad optimization scheme might lead to controversial tool designs but it is worth to show maximal performance that can be achieved on chatter suppression [4] using special tool geometries. The method presented in this work is based on semidiscretization [5], that means, both roughing and finishing opera-

tions are modelled in the optimization scheme adequately.

## GENERAL MILLING PROCESS

In this section the general geometry of a cylindrical cutter is considered with continuous functions. Both radial and helical variations are possible, here. The main purpose is to find the relevant unknowns for a complete optimization scheme to maximize performance. There are obvious problems with this configuration regarding to the toughness of such tools with general geometry. A proper force model is also a problem, which can consider the actual chip flow of such edges.

### General geometry

Basically, the general helix is described by the pitch angle function

$$\varphi_{p,j}(z) = \varphi_{p,j}(0) + \varphi_{\eta,j}(z) - \varphi_{\eta,j+1 \bmod Z}(z), \qquad (1)$$

that contains the difference of the helix lag angle functions of neighbor-hooding edges $j$ and $j+1 \bmod Z$, where $j = 1, 2, ..., Z$.

The actual helix angle can be originated from the helix lag angle function in the following way

$$\tan \eta_j(z) = R_j(z)\, \varphi'_{\eta,j}(z), \qquad (2)$$

\*Address all correspondence to this author.
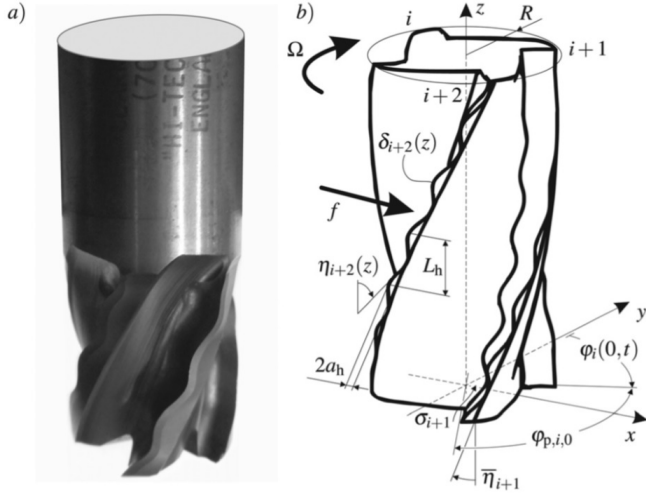
**FIGURE 1**. A real implementation (a) and the sketch (b) of the milling cutter with harmonically varied helix. (The real tool was provided by Prof. Gy. Matyasi: see Acknowledgment.)

considering the radii $R_j(z)$. Variation in the radii changes the lead angle as

$$R'_j(z) = \cot \kappa_j(z). \tag{3}$$

Due to the obvious ring definition of the pitch angles, such as, $\sum_{j=1}^{Z} \varphi_{\mathrm{p},j}(z) = 2\pi$, one of the (first) helix lag angle function is chosen to formulate a complete optimization scheme. Consequently, the edge geometry is uniquely defined if the following functions are known ($i = 1, 2, ..., Z-1$):

$$\varphi_{\mathrm{p},i}(z), \quad \varphi_{\eta,1}(z) \quad \text{and} \quad R_j(z). \tag{4}$$

In this manner all other describing functions can be expressed with (4) according to (2) as

$$\varphi_{\mathrm{p},Z}(z) = 2\pi - \sum_{i=1}^{Z-1} \varphi_{\mathrm{p},i}(z) \quad \text{and}$$
$$\varphi'_{\eta,l}(z) = \sum_{i=1}^{l-1} \varphi'_{\mathrm{p},i}(z) + 2\sum_{k=l}^{Z-1} \varphi'_{\mathrm{p},l}(z) + \varphi'_{\eta,1}(z), \tag{5}$$

with ($l = 2, 3, ..., Z$).

## Regenerative Force

Regeneration of the surfaces is directly originated from the pitch angles due to the constant rotation of the tool with $\Omega$ (see Fig. 1b). Thus

$$\tau_{j,l}(z) = \frac{1}{\Omega} \sum_{k=1}^{l-1} \varphi_{\mathrm{p},(j+k)\bmod Z}(z). \tag{6}$$

In (6) all consecutive arrangements of delays are described to consider the missed-cut effect induced by irregular radii in successive edges. In this way, all possible 'geometric' chip thicknesses can be described as

$$h_{\mathrm{g},j,l}(z,t,\mathbf{r}_t(\theta)) \approx \mathbf{r}_{j,l}(z,t,\mathbf{r}_t(\theta))\mathbf{n}(\varphi_j(z,t)), \tag{7}$$

where the regenerative spatial state of the tool is described by the shift $\mathbf{r}_t(\theta) = \mathbf{r}(t+\theta)$ ($\theta \in [-\tau,0]$, $\tau = \max_{j,l,z} \tau_{j,l}(z)$). The geometric chip thickness in (7) is approximated by the local edge portion movement during $\tau_{j,l}(z)$

$$\mathbf{r}_{j,l}(z,t,\mathbf{r}_t(\theta)) := \mathbf{r}_j(z,t) - \mathbf{r}_{j+l}(z,t-\tau_{j,l}(z)) =$$
$$\Delta\mathbf{r}_{j,l}(t) + \begin{bmatrix} (R_j(z) - R_{j+l\bmod Z}(z))\sin\varphi_j(z,t) + f_{j,l}(z) \\ (R_j(z) - R_{j+l\bmod Z}(z))\cos\varphi_j(z,t) \\ 0 \end{bmatrix}, \tag{8}$$

projected to the local normal $\mathbf{n}$ according to (7) [3]. The so-called regenerative term

$$\Delta\mathbf{r}_{j,l}(t) = \mathbf{r}(t) - \mathbf{r}(t - \tau_{j,l}(z)) \tag{9}$$

describes the difference between the present $\mathbf{r}(t)$ and delayed $\mathbf{r}(t - \tau_{j,l}(z))$ relative motions to the tool holder. The angular position of an edge portion is described with

$$\varphi_j(z,t) = \Omega t + \sum_{k=1}^{j-1} \varphi_{\mathrm{p},k}(z) - \varphi_{\eta,1}(z), \tag{10}$$

while the tool moves $f_{j,l}(z) = v_f \tau_{j,l}(z)$ during one consecutive pass $\tau_{j,l}(z)$ with the secondary 'feed' motion $v_f$ in the $x$ direction (see (8)). By considering the minimum of all possible chip thicknesses the effective one can be derived as according to [6]

$$h_{\mathrm{g},j,e}(z,t,\mathbf{r}_t(\theta)) = \min_{l=1}^{Z} h_{\mathrm{g},j,l}(z,t,\mathbf{r}_t(\theta)). \tag{11}$$

By excluding edge portion passes outside the radial immersion (ri) and the edge portion passes related to missed-cuts (mc) the real chip thickness can be given as

$$h_j(z,t,\mathbf{r}_t(\theta)) = g_j(z,t,\mathbf{r}_t(\theta)) h_{\mathrm{g},j,e}(z,t,\mathbf{r}_t(\theta)), \text{where}$$
$$g_j(z,t,\mathbf{r}_t(\theta)) = g_{\mathrm{ri},j}(z,t)g_{\mathrm{mc},j}(z,t,\mathbf{r}_t(\theta)), \tag{12}$$

where the screen functions $g_j$ are defined with Heaviside step function $H$ as:

$$g_{\mathrm{ri},j}(z,t) = H(\varphi_j(z,t) \bmod 2\pi - \varphi_{\mathrm{en}}) - H(\varphi_j(z,t) \bmod 2\pi - \varphi_{\mathrm{ex}}),$$
$$\text{while} \quad g_{\mathrm{mc},j}(z,t,\mathbf{r}_t(\theta)) = H(h_{\mathrm{g},j,e}(z,t,\mathbf{r}_t(\theta))) \tag{13}$$

The radial immersion is simply described with the entrance and exit angles, $\varphi_{\mathrm{en}}$ and $\varphi_{\mathrm{ex}}$, respectively. The local specific force can be determined in the local $t$ (tangential), $r$ (radial) and $a$ (axial) coordinate system ($tra$), that is,

$$\mathbf{f}_{tra,j}(z,t,\mathbf{r}_t(\theta)) = -(\mathbf{K}_{\mathrm{e}} + \mathbf{K}_{\mathrm{c}} h_j(z,t,\mathbf{r}_t(\theta))),$$

where $\mathbf{K}_{\mathrm{e}}$ and $\mathbf{K}_{\mathrm{c}}$ are the edge and cutting coefficients of the material being cut. The specific force can be rewritten in Cartesian system using the following transformation

$$\mathbf{F}(t,\mathbf{r}_t(\theta)) = -\sum_{j=1}^{Z} \int_0^a g_j(z,t,\mathbf{r}_t(\theta)) \frac{\mathbf{T}(\varphi_j(z,t))\mathbf{f}_{tra,j}(z,t,\mathbf{r}_t(\theta))}{\cos \eta_j(z) \sin \kappa_j(z)} \mathrm{d}z$$

where $\mathbf{T}(\varphi)$ is the transformation matrix [7] between the ($tra$) and the ($xyz$) system.

## Milling Dynamics

General non-proportional dynamics is considered in the following way in space of modal coordinates $\mathbf{q}$

$$\dot{\mathbf{q}}(t) - [\lambda_l]_{l=1}^{2n} \mathbf{q}(\mathbf{t}) = \mathbf{U}^{\mathsf{T}} \mathbf{F}(t,\mathbf{r}_t(\theta)), \tag{14}$$

where $\lambda_k = -\zeta_k \omega_{\mathrm{n},k} + \omega_{\mathrm{d},k}\mathrm{i}$ ($k = 1,2,\ldots,n$ and $\lambda_{n+k} = \overline{\lambda}_k$). The $k$th damped natural angular frequency $\omega_{\mathrm{d},k}$ originates from the undamped one $\omega_{\mathrm{n},k}$ and the modal damping ratio $\zeta_k$ as $\omega_{\mathrm{d},k} = \omega_{\mathrm{n},k}\sqrt{1 - \zeta_k^2}$. The mass normalized modal transformation matrix $\mathbf{U}$ contains $2n$ mode shapes $\mathbf{U}_k$. This transforms the modal coordinates $\mathbf{q}$ to spatial $(x,y,z)$ ones as $\mathrm{col}(\mathbf{r},\dot{\mathbf{r}}) = \mathrm{col}(\mathbf{U}, \mathbf{U}[\lambda_l]_{l=1}^{2n})\mathbf{q}$.

## Linear stability

In order to analyse stability, one can introduce a so-called variational equation [8] 'around' the period-one stationary solution $\mathrm{col}(\mathbf{r}_{\mathrm{P}},\dot{\mathbf{r}}_{\mathrm{P}}) = \mathrm{col}(\mathbf{U}, \mathbf{U}[\lambda_l]_{l=1}^{2n})\mathbf{q}_{\mathrm{P}}$ with time period $T = 2\pi/\Omega$

$$\dot{\mathbf{u}}(t) = [\lambda_l]_{l=1}^{2n} \mathbf{u}(t) + \sum_{j=1}^{Z} \int_0^a \mathbf{C}_j(z,t)(\mathbf{u}(t - \tau_j(z)) - \mathbf{u}(t))\mathrm{d}z, \tag{15}$$

where $\mathbf{q} = \mathbf{q}_{\mathrm{P}} + \mathbf{u}$ and $\mathbf{C}_j(z,t) = \mathbf{C}_j(z,t+T)$. According to the Floquet theory [8], the stability of the linear system (15) is determined by the monodromy operator $U(T)$

$$\mathbf{u}_T(\theta) = (U(T)\mathbf{u}_0)(\theta). \tag{16}$$

The spectrum of the linear operator $U(T)$ consists of so-called characteristic multipliers denoted by $\mu$. If all multipliers lie inside the unit-circle of the complex plane, the time-periodic stationary solution is asymptotically stable. Several semi-analytical methods exist to discretize the operator $U(T)$ and approximate it with a matrix $\Phi$ whose eigenvalues approximate the dominant characteristic multipliers (see [9]). These methods lead to the following form

$$\mathbf{z}_p = \Phi \mathbf{z}_0, \tag{17}$$

where $p \in \mathbb{N}$ is the resolution of the time period, $\mathbf{z}_j = \mathrm{col}_{l=0}^r \mathbf{u}_{t_j}(-l\Delta\theta)$ is the discretized state with $t_0 = 0$, $t_p = T$, $\Delta\theta = \Delta t = T/p$, and $r = \lfloor \tau/\Delta\theta \rfloor$ is the delay resolution. The semidiscretization method (SDM) [5] is one of the simplest among these methods, which serves sufficiently accurate results within reasonable computational time. In this paper, we used SDM to predict SLD's (see figure 2).

## OPTIMIZATION SCHEME

Generally, an optimal edge geometry with the highest 'stable' axial depth of cut values should incorporate, in the parameter region $\Sigma$, with the smallest accumulated maximum magnitude multipliers. In other words, one wants to minimize $\mu_{\max}(z)$ over $(\Sigma, z) \in \mathbb{X}_\Sigma \times [0, a_{\max}]$. By assuming intuitively that $a = 0$ axial depth of cut is stable, the milling tool is actually can be 'built up' from $z = 0$ to an given working length $a_{\max}$.

By considering that every edge geometry segment at $z$ actually affect the spectral behaviour of $\Phi$ (17) the maximal multiplier corresponding to the axial level $z$ has the definition

$$\mu_{\max}(z) :=$$
$$\mu_{\max}(\varphi_{\mathrm{p},i;z}(\zeta), \varphi'_{\mathrm{p},i;z}(\zeta), \varphi_{\eta,1;z}(\zeta), \varphi'_{\eta,1;z}(\zeta), R_{j;z}(\zeta), R'_{j;z}(\zeta)) \tag{18}$$

with the spatially retarded definition $\chi_z(\zeta) = \chi(z+\zeta)$ ($\zeta \in [-z,0]$).

A simple functional can be defined for the optimization over $\mathbb{X}_\Sigma \times [0, a_{\max}]$ in the following way

$$I_\mu := \int_0^{a_{\max}} M_\mu \, \mathrm{d}z = \int_0^{a_{\max}} \int_\Sigma \overline{\mu}_{\max} \mu_{\max} \, \mathrm{d}\Sigma \, \mathrm{d}z, \text{ where}$$
$$M_\mu := M_\mu(\varphi_{\mathrm{p},i;z}(\zeta), \varphi'_{\mathrm{p},i;z}(\zeta), \varphi_{\eta,1;z}(\zeta), \varphi'_{\eta,1;z}(\zeta), R_{j;z}(\zeta), R'_{j;z}(\zeta)). \tag{19}$$

Unfortunately, this definition would lead to a possibly unrealistic tool geometry since there are no constrains defined for the edge describing functions.

In order to have a realistic edge definition the following bounds can be defined

$$\varphi_{p,min} \leq \varphi_{p,j}(z) \leq \varphi_{p,max}, \quad \eta_{min} \leq \eta_j(z) \leq \eta_{p,max}, \tag{20}$$

$$R_{min} \leq R_j(z) \leq R_{max} \quad \text{and} \quad \kappa_{min} \leq \kappa_j(z) \leq \kappa_{max}. \tag{21}$$

These can be summarized in the following eight different inequality conditions:

$$g_{1,j}(\varphi_{p,i}) := \varphi_{p,min} - \varphi_{p,j} \leq 0, \tag{22}$$

$$g_{2,j}(\varphi_{p,i}) := \varphi_{p,j} - \varphi_{p,max} \leq 0, \tag{23}$$

$$g_{3,j}(R_j, \varphi'_{p,i}, \varphi'_{\eta,1}) := \tan\eta_{min} - R_j\,\varphi'_{\eta,j} \leq 0, \tag{24}$$

$$g_{4,j}(R_j, \varphi'_{p,i}, \varphi'_{\eta,1}) := R_j\,\varphi'_{\eta,j} - \tan\eta_{max} \leq 0, \tag{25}$$

$$g_{5,j}(R_j) := R_{min} - R_j \leq 0, \tag{26}$$

$$g_{6,j}(R_j) := R_j - R_{max} \leq 0, \tag{27}$$

$$g_{7,j}(R'_j) := \cot\kappa_{min} - R'_j \leq 0, \tag{28}$$

$$g_{8,j}(R'_j) := R'_j - \cot\kappa_{max} \leq 0. \tag{29}$$

By considering the Karush-Kuhn-Tucker optimization scheme the inequality conditions in (29) can be included in the functional (19) by introducing Lagrange multipliers $\lambda_{k,j}$ and slack variables $s_{k,j}$ ($r$ is even) as

$$M := M_\mu + \sum_{k=1}^{8}\sum_{j=1}^{Z}\lambda_{k,j}(g_{k,j} + s_{k,j}^r). \tag{30}$$

The minimum of the kernel in (30) is granted over $z \in [0, a_{max}]$ by considering the variation of the effect function $I := \int_0^{a_{max}} M\,\mathrm{d}z$ as $\delta I = 0$. The variational calculus lead to Fréchet derivatives w.r.t. the shifted unknown functions defined in (18) resulting in an Euler-Lagrange formalism. The retarded functional $I$ has a minimum when the differential algebraic equation in (31) is satisfied

$$
\left.
\begin{aligned}
&\vdots_{i=1,2,\dots,Z-1}\\[2pt]
\int_{-z}^{0}(H_z(\vartheta) - H_z(a_{max}+\vartheta))\left(\frac{\partial M_\mu(z-\vartheta)}{\partial \varphi_{p,i;z}(\vartheta)} - \frac{\mathrm{d}}{\mathrm{d}z}\frac{\partial M_\mu(z-\vartheta)}{\partial \varphi'_{p,i;z}(\vartheta)}\right)\mathrm{d}\vartheta + \sum_{j=1}^{Z}\sum_{k=1}^{2}\lambda_{k,j}(z)\frac{\partial g_{k,j}(z)}{\partial \varphi_{p,i;z}(0)} - \lambda_{k+2,j}(z)\frac{\mathrm{d}}{\mathrm{d}z}\frac{\partial g_{k+2,j}(z)}{\partial \varphi'_{p,i;z}(0)} = 0,\\[4pt]
\int_{-z}^{0}(H_z(\vartheta) - H_z(a_{max}+\vartheta))\left(\frac{\partial M_\mu(z-\vartheta)}{\partial \varphi_{\eta,1;z}(\vartheta)} - \frac{\mathrm{d}}{\mathrm{d}z}\frac{\partial M_\mu(z-\vartheta)}{\partial \varphi'_{\eta,1;z}(\vartheta)}\right)\mathrm{d}\vartheta - \sum_{j=1}^{Z}\sum_{k=3}^{4}\lambda_{k,j}(z)\frac{\mathrm{d}}{\mathrm{d}z}\frac{\partial g_{k,j}(z)}{\partial \varphi'_{\eta,1;z}(0)} = 0,\\[4pt]
&\vdots_{j=1,2,\dots,Z}\\[2pt]
\int_{-z}^{0}(H_z(\vartheta) - H_z(a_{max}+\vartheta))\left(\frac{\partial M_\mu(z-\vartheta)}{\partial R_{j;z}(\vartheta)} - \frac{\mathrm{d}}{\mathrm{d}z}\frac{\partial M_\mu(z-\vartheta)}{\partial R'_{j;z}(\vartheta)}\right)\mathrm{d}\vartheta + \sum_{j=1}^{Z}\sum_{k=3}^{6}\lambda_{k,j}(z)\frac{\partial g_{k,j}(z)}{\partial R_{j;z}(0)} - \sum_{k=7}^{8}\lambda_{k,j}(z)\frac{\mathrm{d}}{\mathrm{d}z}\frac{\partial g_{k,j}(z)}{\partial R'_{j;z}(0)} = 0,\\[4pt]
&\vdots_{k=1,2,\dots,8,\,j=1,2,\dots,Z}\\[2pt]
g_{k,j}(z) + s_{k,j}^r(z) = \varepsilon\,s'_{k,j}(z),\\[4pt]
&\vdots_{k=1,2,\dots,8,\,j=1,2,\dots,Z}\\[2pt]
r\lambda_{k,j}(z)s_{k,j}^{r-1}(z) = 0.
\end{aligned}
\right\} \tag{31}
$$

The equation system theoretically can be solved over $z \in [0, a_{max}]$ by considering the initial conditions

$$
\begin{aligned}
&\varphi_{p,i;0}(0) := \varphi_{p,i,0}, \quad \varphi'_{p,i;0}(0) := d\varphi_{p,i,0}, \quad \lambda_{k,j}(0) := 0,\\
&R_{j;0}(0) := R_{j,0}, \quad\quad R'_{j;0}(0) := dR_{j,0}, \quad s_{k,j}(0) :\neq 0,\\
&\varphi_{\eta,1;0}(0) := \varphi_{\eta,1,0}, \quad \varphi'_{\eta,1;0}(0) := d\varphi_{\eta,1,0}.
\end{aligned} \tag{32}
$$

The inequality conditions in (29) are too stiff bounds for such optimization as tool geometry. Obviously, tool geometry can not satisfy the conditions abruptly, that is, a singular perturbation is introduced by $\varepsilon$ for their algebraic conditions. The singular perturbation allows to approach the bounds in a more elastic manner avoiding immediate change in the continuous unknown functions defined in (4)
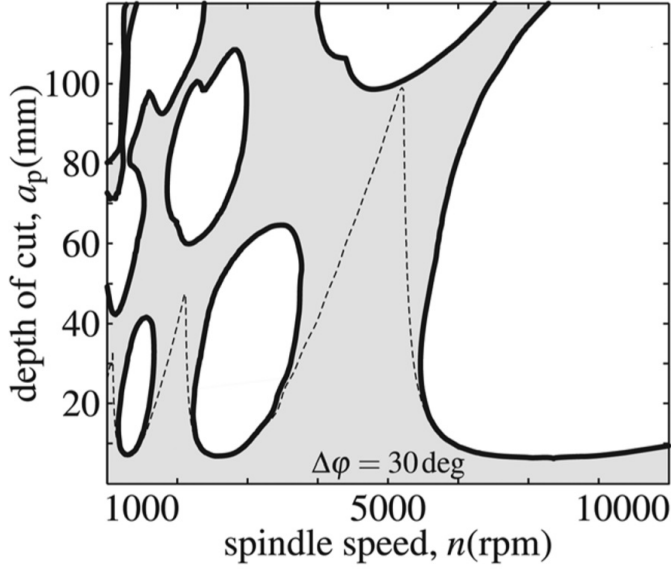
**FIGURE 2**. Stability Lobe Diagram (SLD) of a variable helix cutter [10].

## DIFFERENTIAL FORMS

The multipliers are the eigenvalues of the transition matrix $\Phi$, thus

$$(\Phi - \mu \mathbf{I})\,\mathbf{s} = \mathbf{0} \quad \Rightarrow \quad (\mu_{\max}, \mathbf{s}_{\max}) = (\mu_k, \mathbf{s}_k) \quad \text{for such } k, \text{ where } |\mu_{\max}| := \max_k |\mu_k|. \tag{33}$$

By using the corresponding eigenvector $\mathbf{s}_{\max}$ to $\mu_{\max}$ the derivatives in (31) can be derived as

$$\frac{\partial M_\mu}{\partial \alpha} = \mathbf{s}_{i,\max}^\mathsf{T} \frac{\partial \Phi}{\partial \alpha} \mathbf{s}_{\max}, \quad \frac{\mathrm{d}}{\mathrm{d}z} \frac{\partial M_\mu}{\partial \beta} = \mathbf{s}_{i,\max}^\mathsf{T} \frac{\mathrm{d}}{\mathrm{d}z} \frac{\partial \Phi}{\partial \beta} \mathbf{s}_{\max},$$
$$\text{where } \mathbf{S}^{-1} = (\mathrm{row}_k\, \mathbf{s}_k)^{-1} = \mathrm{col}_k\, \mathbf{s}_{i,k}^\mathsf{T}, \text{ and}$$
$$\alpha = \varphi_{\mathrm{p},i;z}(\zeta), \varphi_{\eta,1;z}(\zeta), R_{j;z}(\zeta), \beta = \varphi_{\mathrm{p},i;z}'(\zeta), \varphi_{\eta,1;z}'(\zeta), R_{j;z}'(\zeta). \tag{34}$$

These derivatives can be determined numerically and the equation in (31) can be simulated by using a stiff solver. Regardless of the actual geometry, the simulation of (31) can be enormous considering that in each step the derivatives must be calculated for all unknown function (4) for all retarded positions in the interval $\zeta \in [-z, 0]$.

## CONCLUSIONS

This work was motivated to find the best possible edge geometry to maximize stability for a certain milling operation. The necessary equations were derived in order to perform a simulation based edge build-up, which results in the optimal geometry under feasibility conditions. These conditions can ensure the manufacturability of such tool optimized by the scheme presented. In this work we used the retarded definition for a functional for which the corresponding Euler-Lagrange differential formalism was derived.

## REFERENCES

[1] Stepan, G., Hajdu, D., Iglesias, A., Takacs, D., and Dombovari, Z., 2018. "Ultimate capability of variable pitch milling cutters". *CIRP Annals, accepted*, pp. 1–4.

[2] Dombovari, Z., and Stepan, G., 2011. "The effect of harmonic helix angle variation on milling stability". In ASME IDETC/CIE 2011, Washington, DC, USA.

[3] Dombovari, Z., Altintas, Y., and Stepan, G., 2009. "Stability of serrated milling cutters". In 12th Cirp Conference on Modelling of Machining Operations. Donostia-San Sebastian, Spain, May 7-8.

[4] Munoa, J., Beudaert, X., Dombovari, Z., Altintas, Y., Budak, E., Brecher, C., and Stepan, G., 2016. "Chatter suppression techniques in metal cutting". *CIRP Annals - Manufacturing Technology,* **65**(2), pp. 785–808.

[5] Insperger, T., and Stepan, G., 2011. *Semi-Discretization for Time-Delay Systems: Stability and Engineering Applications*. Springer, New York.

[6] Wang, J.-J., and Liang, S. Y., 1996. "Chip load kinematics in milling with radial cutter runout". *Journal of engineering for industry,* **118**, pp. 111–116.

[7] Dombovari, Z., Altintas, Y., and Stepan, G., 2010. "The effect of serration on mechanics and stability of milling cutters". *International Journal of Machine Tools and Manufacture,* **50**(6), pp. 511 – 520.

[8] Farkas, M., 1994. *Periodic Motions*. Springer-Verlag, Berlin and New York.

[9] Lehotzky, D., and Insperger, T., 2016. "A pseudospectral tau approximation for time delay systems and its comparison with other weighted residual type methods". *Int. J. Numer. Meth. Eng.,* **108**(6), pp. 588–613.

[10] Dombovari, Z., and Stepan, G., 2012. "The effect on helix angle variation on milling stability". *Journal of Manufacturing Science and Engineering,* **134(5)**, pp. 051015(1)–051015(6).